Atmospheric Environment 237 (2020) 117668

Contents lists available at ScienceDirect

Atmospheric Environment

journal homepage: http://www.elsevier.com/locate/atmosenv

Iron and steel industry emissions and contribution to the air quality in China

Ling Tang [a,b], Xiaoda Xue [a,c], Min Jia [b,c], Hong Jing [d], Tong Wang [e], Ruiqing Zhen [f], Mantang Huang [g], Jun Tian [g], Jing Guo [a,c], Ling Li [h], Xin Bo [c,*], Shouyang Wang [i]

[a] School of Economics and Management, Beihang University, Beijing, 100191, China
[b] School of Economics and Management, Beijing University of Chemical Technology, Beijing, 100029, China
[c] Appraisal Center for Environment and Engineering, Ministry of Ecology and Environment, Beijing, 100012, China
[d] China National Environmental Monitoring Centre, Beijing, 100012, China
[e] Shaanxi Environmental Investigation and Assessment Center, Xian, 710000, China
[f] Capital Engineering & Research Incorporation Limited, Beijing, 100176, China
[g] Academy of Environmental Planning & Design, Co., Ltd, Nanjing University, Nanjing, 210093, China
[h] International School of Economics and Management, Capital University of Economics and Business, Beijing, 100070, China
[i] Academy of Mathematics and Systems Science, Chinese Academy of Sciences, Beijing, 100190, China

HIGHLIGHTS

- Impact of China's iron and steel industry emissions on air quality is simulated.
- Sintering and pelletizing presented the largest emission intensities.
- The largest contributors were mainly concentrated in eastern China.
- SO_2 made the largest contribution to air quality in iron and steel industry.
- Emission sources presented the greatest contribution to air quality concentration in summer.

ARTICLE INFO

Keywords:
Iron and steel industry
China
Air quality
CAMx

ABSTRACT

To reduce the emissions from the iron and steel industry, China has imposed a series of strengthened emission standards since 2012. An accurate impact of emission reduction on the air quality is critical for evaluating policy efficiency. This study was the first attempt to explore the contribution of emissions from China's iron and steel industry to ambient air quality at national scale, after the implementation of current standards in 2012. First, all emission sources in production processes were estimated at unit level in China's iron and steel industry, covering sulfur dioxide (SO_2), nitrogen oxides (NOx) and particulate matter ($PM_{2.5}$), etc. Second, the corresponding air quality impacts were modeled with the Comprehensive Air Quality Model with extensions (CAMx) model. We find that emission hotspots from China's iron and steel industry, with following aspects. (1) From a spatial perspective, the largest emissions and ambient concentration contributors were mainly concentrated in eastern areas of China, with high crude steel production. (2) Among three main pollutants (i.e., SO_2, NOx and $PM_{2.5}$), SO_2 made the largest contribution to ambient concentration in China's iron and steel industry. (3) As for temporal distribution, emission sources presented the greatest contribution to air quality concentration in summer. (4) For policy evaluation, under the current standards in 2012, the contribution of iron and steel industry emissions to air quality decreased by 92.07% and 72.91% for SO_2 and $PM_{2.5}$, respectively. Therefore, these results will be essential to reflecting current emission characteristics and underscoring further opportunities for emission reductions.

* Corresponding author.
E-mail address: boxin@acee.org.cn (X. Bo).

https://doi.org/10.1016/j.atmosenv.2020.117668
Received 3 December 2019; Received in revised form 30 May 2020; Accepted 1 June 2020
Available online 5 June 2020
1352-2310/© 2020 Elsevier Ltd. All rights reserved.

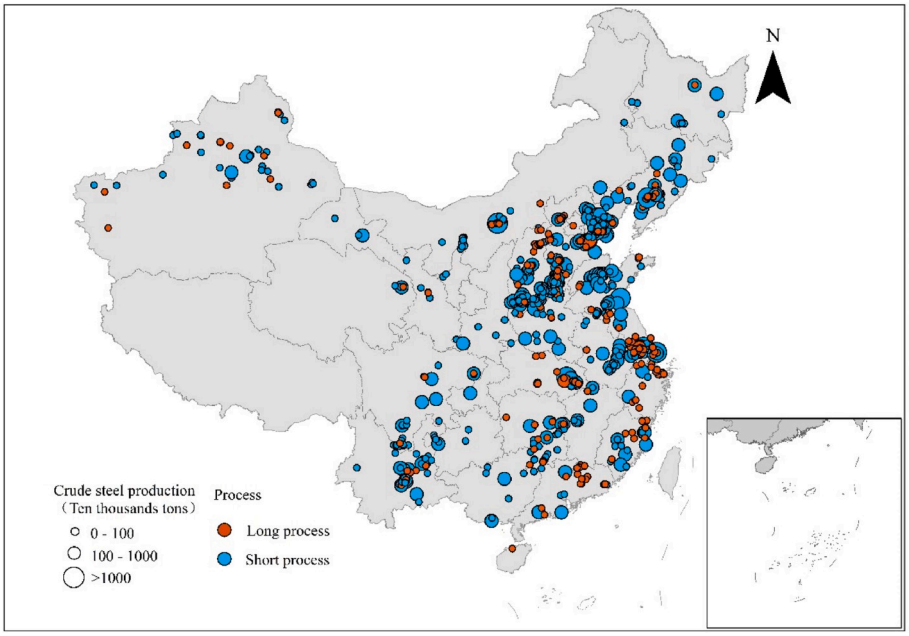


Fig. 1. China's iron and steel industry locations and distribution of crude steel production.

Table 1
Mass percentage of $PM_{2.5}$ in PM_{10} (%).

Coking	Sintering			Pelletizing	BF		BOF		EAF	Steel Rolling
Quenching	30.46[1]	Head	56.07[1]	43.37[2]	Casting	62.94[1]	Hot metal pretreatment	45.06[1]	74.14[2]	62.51
Coal preparation	37.78[1]	Tail	51.11[1]		Ore tank	15.27[1]	Secondary off gas	56.68[1]		
Coal charging& Pushing	40.97[1]	Raw material preparation	36.62[1]		Others	62.51[2]	Primary off gas	71.43[2]		
Coke oven chimney	40.97[1]	Size stabilization system	38.63[1]		–	–	Underground bunker	71.43[2]		

[1]Zhang (2015),[2]He (2017).

Table 2
Emission factors of pollutants in different processes in 2012 (Unit: kg/t for VOCs and CO, ng I-TEQ/t for PCDD/Fs, and % for BC, OC and EC (the percentage of $PM_{2.5}$)).

Pollution	PCDD/Fs	VOCs	CO	BC	OC	EC	F
Coking	324.4[2]	2.96[1]	1.6[1]	30[6]	35[6]	_	_
Sintering	8000[2]	0.25[1]	22[6]	1[6]	2.2[8]	0.4[7]	0.0028[2]
Pelletizing	196[2]	0.25[1]	0.064	1[6]	2.2[7]	0.4[7]	0.0009[2]
Blast furnace	2[2]	_	22.3[6]	10[6]	6.2[7]	0.8[7]	_
BOF	690[2]	0.06[1]	35.2[6]	1.175[6]	8.8[7]	0.7[7]	0.0065[2]
EAF	3000[2]	0.1[5]	9[1]	14.19[6]	8.8[7]	0.7[7]	0.0031[2]
Hot rolling	_	0.3[3]	1.28[1]	1.175[6]	8.8[7]	0.7[7]	_
Cold rolling	_	0.062[4]	_	_	_	_	_

[1]He (2017), [2]Our field investigation,[3]MEE (2014), [4]Wu et al. (2015), [5]Liu et al. (2018),[6]Lei (2008), [7]Wen et al. (2018).

Table 3
CAMx model configurations.

Process	Method	Reference
Horizontal advection	PPM	Colella and Woodward (1984)
Vertical diffusion	Standard K Theory	ENVIRON (2016)
Dry settlement parameterization scheme	WESELY89	Wesely (1989)
Chemical mechanism of liquid phase	RADM-AQ	ENVIRON (2016)
Gas phase chemical mechanism	SAPRC99	Colella and Woodward (1984)
Aerosol module	CF Scheme	ENVIRON (2016)
Thermodynamic equilibrium model of aerosol	ISORROPIA	Nenes et al. (1998)

Table 4
CAMx modelling scenarios.

Scenario	Emissions	Year
S-0	Background emissions	2012
S-1	Background emissions + iron and industry emissions	2012

1. Introduction

In recent decades, with the boom in infrastructure construction, the increases in China's iron and steel industry emissions have led to degradation of the ambient air quality and associated human health problems. China has become the largest steel producer in the world, accounting for 51.88% of the word's crude steel production in 2018 (approximately 5.66 times above the figures for 1990) (World Steel Association, 1990–2019). Though vital to China's economy, as one of the most emission-intensive sectors (Zhao et al., 2011; Zheng et al., 2018), massive amounts of air pollutants have been emitted from the iron and steel industry (Kim et al., 2016; Li et al., 2017; Tan et al., 2017).

In particular, the industry has contributed 11.15%, 8.83% and 28.98% to Chinese anthropogenic emissions of sulfur dioxide (SO_2), nitrous oxides (NO_X) and particulate matter (PM) in 2015 (MEE, 2016), respectively, and surpassed 30% of Chinese polychlorinated dibenzo-p-dioxins and polychlorinated dibenzofurans (PCDD/Fs) emissions in 2004 (MEPFECO, 2007). As a result, these emissions have led to air quality degradation (e.g., atmospheric haze and acid rain) (Dai et al.,

Table 5
Statistical indicators for comparison of simulated and monitoring data for $PM_{2.5}$.

	R	FB (%)	NMB (%)	NME (%)
Beijing	0.87	−31.08	−29.80	40.61
Shanghai	0.63	−4.77	−4.43	45.76
Guangzhou	0.27	−52.55	−47.79	60.74
Chengdu	0.68	31.45	7.01	33.86

Table 6
Statistical indictors for comparison of simulated and monitoring data for PM_{10}, SO_2 and NOx.

	R	FB (%)	NMB (%)	NME (%)
PM_{10}	0.58	14.74	−13.72	51.78
SO_2	0.63	19.06	−17.40	47.75
NOx	0.63	4.64	−4.54	37.61

2016; Huang et al., 2014; Li et al., 2016; Zhao et al., 2012) and human health problems (e.g., respiratory diseases, cardiovascular diseases, breast cancer and premature deaths) (Chen et al., 2013; Coudon et al., 2019; Ho et al., 2016; Shutt et al., 2017; Zheng et al., 2018). To tackle these problems, it is essential to explore the contribution of China's iron and steel industry emissions to the ambient air quality.

To address air pollution in the iron and steel industry, China has introduced a series of strengthened emission standards in October 1, 2012 (shown in Supplementary Table 1). These compulsory standards cover all production process of iron and steel industry. In particular, for the sintering process (i.e., the most important process for emissions), the current standards are ambitious, with levels of stringency surpassing the previous standards (i.e., GB 16297–1996) by up to 91% and 60% for SO_2 and PM, respectively. To comply with these tightened standards, penetrations of highly efficient pollutant control technologies are actively promoted (e.g., flue gas desulfurization and high-efficiency PM control facilities) (Guo et al., 2017; Wang et al., 2019). Consequently, pollutant concentrations are dramatically decreased and effectively controlled within standard limits (Zhang et al., 2009; Zheng et al., 2018). Under such a background, the implementation of these standards has greatly reduced emissions from the iron and steel industry since 2012. To reflect the impact of the emission standards implemented in 2012, this paper attempts to explore the contribution of China's iron and steel industry emissions to ambient air quality.

However, the research on contributions of China's iron and steel industry emissions to the air quality concentration at the national scale is still lacking. The existing research has mainly focused on three different scales: local, city and regional (Acciai et al., 2017; Bo et al., 2017; Di Gilio et al., 2017). For the local scale, the identification and apportionment of emission sources of airborne PM concentrations in the vicinity of the integrated steelworks complex has been conducted (Dai et al., 2016). At the city scale, the contributions of iron and steel industry emissions to the ambient environment (i.e., $PM_{2.5}$ or PM_{10} concentration) have been explored in different cities; for example, in Beijing (Jia et al., 2018; Song et al., 2006), Shanghai (Tan et al., 2015), Xi'an (Huang et al., 2014), Wuhan (Acciai et al., 2017) and Lanzhou (Tan et al., 2017). At the regional scale, the magnitude of the iron and steel industry emissions contribution to airborne $PM_{2.5}$ concentrations in the Beijing–Tianjin–Hebei region has been simulated (Bo et al., 2017; Duan et al., 2018). Therefore, this study aims to fill in the literature gap for the national level and explore the contribution of China's iron and steel industry emissions to the air quality nationwide in 2012.

In terms of analytical techniques, source apportionment methods can be generally divided into source-oriented and receptor-oriented models. In particular, receptor-oriented models measure mass of source tracers at both a given site (i.e., receptor) and emission sources, and adopt statistical analysis method to obtain quantitative contributions of each emission source (Almeida et al., 2015; Salameh et al., 2016; Taiwo et al., 2014). Though highly accurate, this method might be somewhat limited in terms of spatial coverage, with only contribution at the specific given site (i.e., receptor) obtained (Almeida et al., 2015; Guo et al., 2017). In comparison, source-oriented models, relying on emission inventory and meteorological field, account for emission transport at the large scale and thus effectively solve these problems (Ciarelli et al., 2017). Thus, source-oriented models have been applied to simulate iron and steel industry emissions impacts on air quality, such as the Comprehensive Air Quality Model with extensions (CAMx) (Fann et al., 2012), Community Multiscale Air Quality model (CMAQ) (Jia et al., 2018) and California Puff model (CALPUFF) (Abdul-Wahab et al., 2018; Gulia et al., 2015). Among these models, CALPUFF is more suitable for simulation at city or provincial level (Abdul-Wahab et al., 2018). Both CMAQ and CAMx show good overall performance, without systematic superiority over each other at the national scale (Shen et al., 2011; Tesche et al., 2006). Indeed, our previous studies have verified the good performance of CAMx in air quality simulation in China (Bo et al., 2017, 2019; Du et al., 2016; Wang et al., 2016a). Specifically, CAMx particularly involves "one-atmosphere" assessment of multi-pollutants impacts during atmospheric transportation, including physical and chemical processes (Ciarelli et al., 2017), and thus has widely been employed to quantify the contributions of iron and steel industry emissions; for example, in the US (Fann et al., 2012), China (Bo et al., 2017; Duan et al., 2018) and India (Guttikunda et al., 2019). Therefore, this study employed the CAMx model to explore air quality impacts.

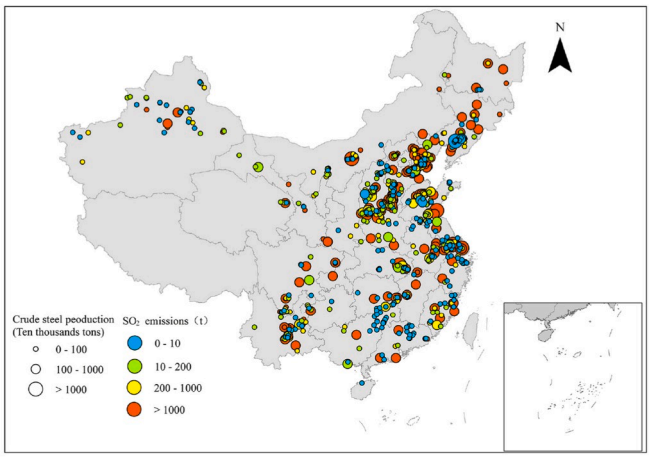
The CAMx model requires a well-established inventory for China's iron and industry emissions. However, existing studies only examined the emissions of iron and steel industry before 2012 in China (Lei et al., 2011; Wang et al., 2016b; Zhao et al., 2013). Although some inventories were established after 2012, they only focused on provincial-level (Wu et al., 2015), annual-frequency (Wu et al., 2015), a certain process (Zheng et al., 2018) and a certain pollutant (e.g., SO_2, NOx and PM) (Wang et al., 2019). Therefore, this study attempts to fill the literature gaps by providing an updated and high-resolution (i.e., unit-based, monthly-frequency, source-level and multi-pollutant) emissions inventory for China's iron and steel industry in 2012.

To the best of our knowledge, this study is the first attempt to explore the contribution of China's iron and steel industry emissions to the ambient air quality at the national level. The major innovations of this study can be summarized into the following three aspects: (1) a first attempt to investigate the impact of China's iron and steel industry emissions on air quality at the national scale; (2) based on updated emission factors, a high-resolution emission inventory of iron and steel industry at a national scale was constructed for 2012; (3) by introducing the new emission inventory into the CAMx model, the air quality improvement of emission standards implementation for China's iron and steel industry in 2012 were systematically simulated.

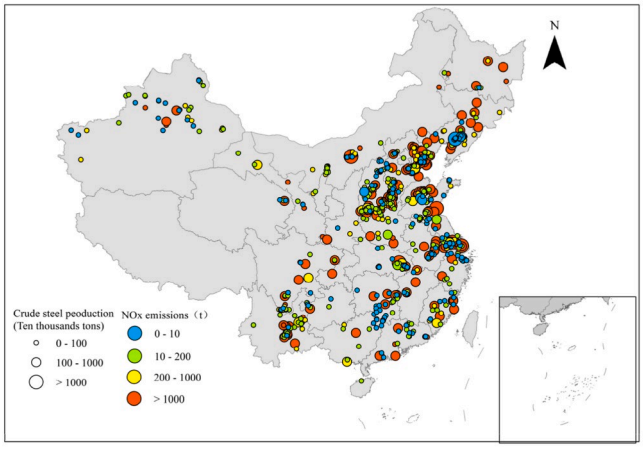
The main aim of this research was to explore overall impact of

Table 7
Results of linear regression analyses on the relationship of economic level and iron and steel industry environmental impacts.

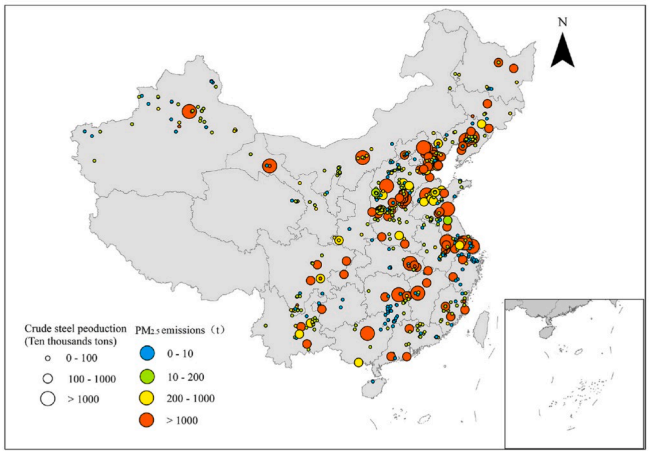
Variable	Model 1 (Y is SO_2; Fig. 3(a))				Model 2 (Y is NO_X; Fig. 3(b))				Model 3 (Y is $PM_{2.5}$; Fig. 3(c))			
	Coeff.	*t*-stat.	*p*-value	Std.	Coeff.	*t*-stat.	*p*-value	Std.	Coeff.	*t*-stat.	*p*-value	Std.
GDP	−0.13***	3.04***	0.01	0.04	−0.09***	−3.24***	0.00	0.03	−0.02***	−3.32***	0.00	0.01
N	28				28				28			
F-stat.	9.28***				10.53***				11.02***			



(a) SO_2 emissions



(b) NO_X emissions



(c) $PM_{2.5}$ emissions

Fig. 2. Spatial distributions of China's iron and steel industry emission for SO_2 (a), NO_X (b) and $PM_{2.5}$ (c).

China's iron and steel industry emissions on air quality. The remainder of the paper is organized as follows. The methods for emission inventory and air quality simulation are illustrated in Section 2. The contribution results are thoroughly analyzed, and policy suggestions can be obtained for iron and industry emission control in Section 3. Section 4 concludes the paper and outlines the possible directions of future research.

2. Methodology

This study explored the contribution of emissions from China's iron and steel industry to air quality, based on the CAMx model version 6.4, a three-dimensional air quality model (Ciarelli et al., 2017), and provided a nationwide, unit-based inventory of China's iron and steel industry emissions in 2012.

Accordingly, two main steps were involved in this research. First, an updated emission inventory with high resolutions was constructed for China's iron and steel industry, including SO_2, NO_X, PM_{10}, $PM_{2.5}$, carbon monoxide (CO), black carbon (BC), organic carbon (OC), elemental carbon (EC), volatile organic carbons (VOCs), PCDD/Fs and fluoride (F), based on the unit bottom-up method. Second, the corresponding impact on air quality was simulated with the CAMx model. The two major steps are presented in Sections 2.1 and 2.2, respectively, with details of the corresponding analytical techniques.

2.1. Emission estimation

China's iron and steel industry emission inventory encompasses 1499 iron and steel enterprises in the 26 Chinese provinces and 4 municipalities, excluding Hong Kong, Macao, Taiwan and Tibet. These enterprises consist of 739 long processes (i.e., producing crude steel from iron ore and coke in the melted and conversion process) and 760 short processes (i.e., employing steel scrap as a raw material to melt steel directly) (Wu et al., 2017; Zhu et al., 2019). In total, the processes of iron and steel production involved in this study include emissions from coking, sintering, pelletizing, iron-making (i.e., blast furnace), steel-making (i.e., converter furnace and electric furnace), rolled steel (i.e., hot rolling and cold rolling), with 265 coke ovens, 1088 sintering machines, 631 pellet-firing machines, 3674 blast furnaces, 791 converter furnaces and 406 electric furnaces, respectively. Incorporated crude steel production in the analysis reaches 677 million tons, accounting for 92.58% of total national crude steel production. Fig. 1 presents the geographic locations and crude steel productions of iron and steel enterprises in China.

2.1.1. Unit-based bottom-up methodology

In this study, a unit-based bottom-up approach was adopted to calculate China's iron and steel industry emissions. Based on the emission factor methods, emissions from each iron and steel unit were calculated separately and then aggregated to obtain city-, provincial- and regional-level emissions (Wang et al., 2016c).

Absolute multi-pollutant emissions (SO_2, NO_X, PM_{10}, $PM_{2.5}$, CO, BC, OC, EC, VOCs, PCDD/Fs and F) of each iron and steel unit were estimated by multiplying the activity level by the associated emission factors (Liu et al., 2015):

$$E_{s,i,p,m} = A_{i,p,m} EF_{s,i,p}, \quad (1)$$

where the subscripts s, i and p indicate the emission pollutant, unit and process, respectively; m indicates the month; E represents the unit-based emissions, emitted from iron and steel production (g), and A is the activity level, defined as the amount of production for each process (kg for sintering process, pellet process, steel-making process and rolling process), and EF is the emission factor, that is, the mass of emissions per unit of production (g/kg). In this research, iron and steel industry emissions were estimated at a monthly scale. The annual activity rates at the unit level were available, and thus we used the monthly crude steel

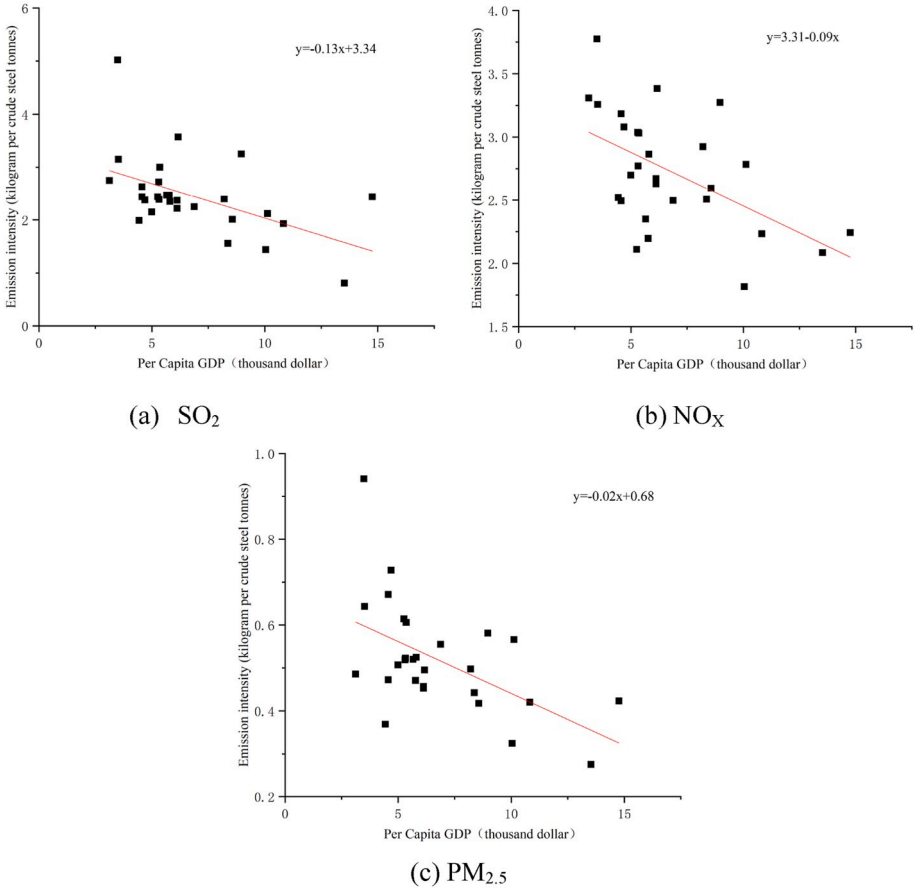


Fig. 3. China's iron and steel industry emission intensity for SO_2 (**a**), NOx (**b**) and $PM_{2.5}$ (**c**) with GDP for 28 provinces or municipalities in 2012.

production as a surrogate to allocate the monthly activity rate (A) at the unit level:

$$A_{i,y,m} = \frac{F_{k_i,y,m}}{\sum_{m=1}^{12} F_{k_i,y,m}} A_{i,y}, \quad (2)$$

where k_i indicates the province of unit i and F is the province-level crude steel production that is available in the statistics (National Bureau of Statistics, 2013).

2.1.2. Activity level

The updated activity data were obtained from the facility-level survey data of the Ministry of Ecology and Environment (MEE) (unpublished data). This database contains 1499 integrated iron and steel enterprises, with detailed information about production, geographical location, air pollution control measurements and equipment scale in 2012. In particular, productions at specific unit level contain coke production, sinter ore production, pellet production, steel-making production for converter furnaces and electric furnaces, and rolled steel production for hot rolling and cold rolling. Furthermore, the geographical location of each iron and steel enterprise was individually validated by using Google Earth.

2.1.3. Emission factors

In general, emission factors of SO_2, NO_X and PM_{10}, were estimated according to the technology-based method. Emission factors of CO, BC, OC, EC, VOCs, PCDD/Fs and F were obtained from previous studies (listed in Table 1 and Table 2).

2.1.3.1. Emission factors of SO_2, NO_X and PM_{10}. To improve the accuracy of the inventory, all emission sources in production processes were classified in terms of production, equipment scale and pollution control technology (shown in Tables S1–S6). Different categories are relative to corresponding concentrations and theoretical flue gas rate (Bo et al., 2015).

As for classification of emission sources, sinter machine head and pellet firing were classified in terms of the presence of desulfurization and denitrification facilities; blast furnace, basic oxygen furnace, electric arc furnace and other emission sources of sintering were classified in terms of the equipment scale; coking and other emission sources of pelletizing were classified in terms of the capacity. The emission sources with large scales or capacities and high removal efficiency of control technology were classified as Level 1; the emission sources with small scale or capacity and low removal efficiency of control technology were classified as Level 3; and the other emission sources were classified as Level 2. In particular, the classification of emission sources scale in iron and steel production was from National Development and Reform Commission (NDRC, 2013).

For the establishment of emission factor database, the emission factors (SO_2, NO_X, PM_{10}) of emission sources of different scales were calculated by multiplying the corresponding concentration by theoretical flue gas rate (Bo et al., 2015):

$$EF_{s,i,p} = C_{s,i,p} V_{s,i,p}, \quad (3)$$

where C represents the unit-based concentrations, emitted from iron and steel production (mg/m^3), and V means the theoretical flue gas rate, which is expressed as the volume of flue gas per unit of production (m^3/t).

Among them, the concentration values were obtained from the existing, new and special emission concentration limits in the relevant current standards (i.e., GB 28662–2012, GB 28663–2012, GB

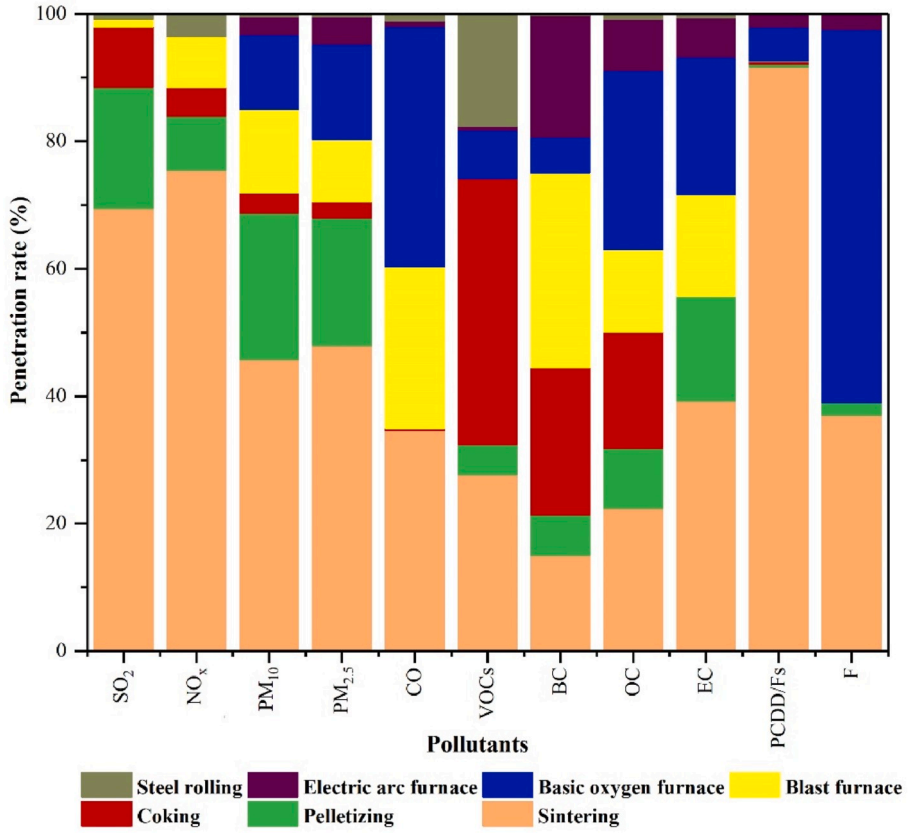


Fig. 4. Contribution of emissions from different processes in China's iron and steel industry in 2012.

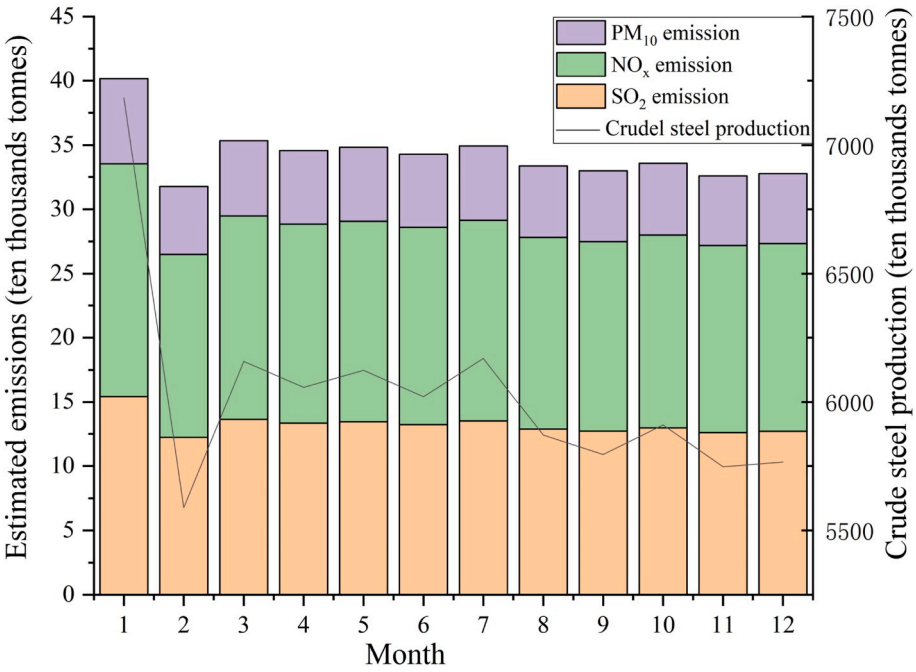


Fig. 5. Monthly emissions and crude steel production from China's iron and steel industry in 2012.

28664–2012, GB 28665–2012 and GB 16171–2012; Tables S1–S6). Level 3 corresponds to the concentration limit for the existing plant; Level 2 corresponds to the concentration limit for a new plant and Level 1 corresponds to the special concentration limit. The flue gas rates for the different classifications were obtained from the Ministry of Ecology and Environment (MEE, 2017a) (Tables S1–S6).

2.1.3.2. Emission factors of other pollutants. Other pollutants included $PM_{2.5}$, BC, OC, EC, PCDD/Fs, VOC, CO and F. The emissions of $PM_{2.5}$ were calculated based on the emissions of PM_{10} and the mass

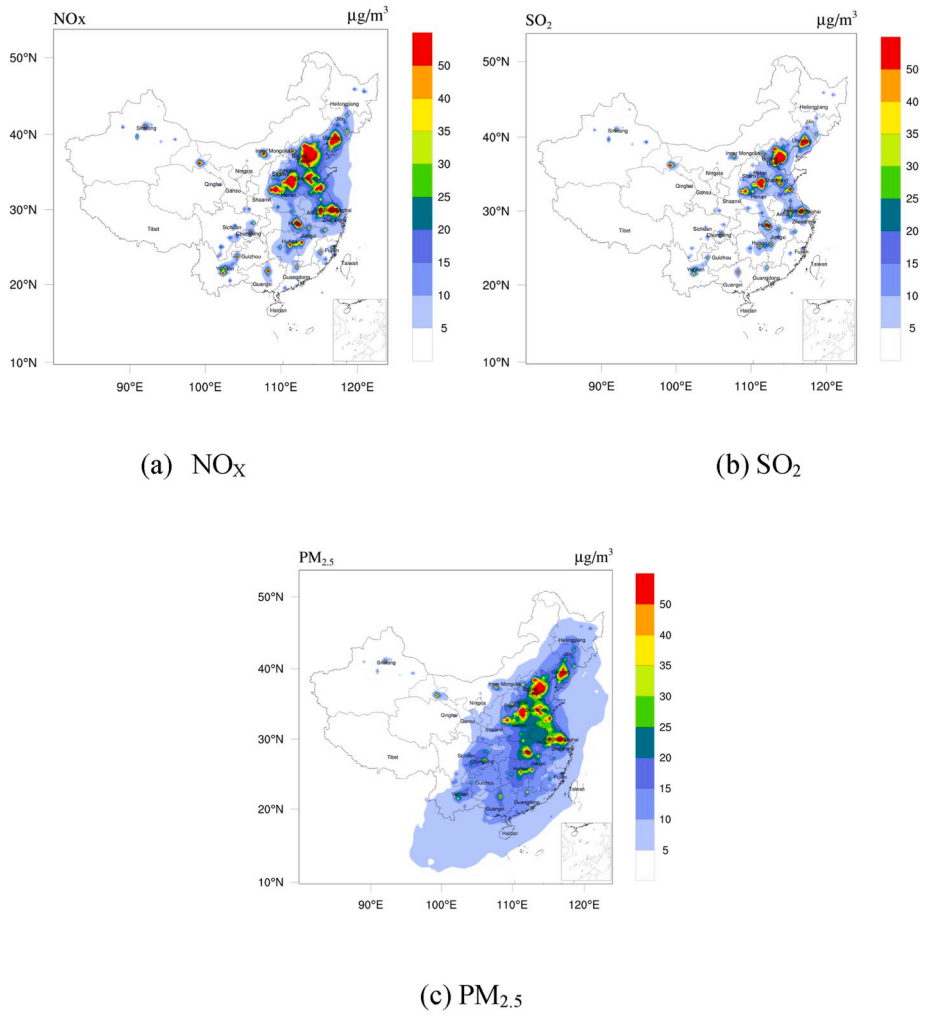


Fig. 6. Contribution of air pollutants emitted by China's iron and steel industry to ambient concentration in 2012 in terms of incremental concentrations (µg/m^3).

percentages of $PM_{2.5}$ in PM_{10} in different processes. The mass percentages of $PM_{2.5}$ in PM_{10} were obtained from the previous literature, as shown in Table 1. The pollutant emission factors of BC, OC, EC, PCDD/Fs, VOC, CO and F for each production process in the iron and steel industry were obtained from previous literature (Table 2).

2.1.4. Uncertainty analysis

An uncertainty analysis was conducted to verify the reliability of emission estimation, based on the Monte Carlo approach. First, as an important input, the activity data should be considered in the uncertainty analysis. Accordingly, the probability of unit-specific production is assumed to obey a normal distribution with coefficients of variation (CV, the standard deviation divided by the mean) of 5% (Wang et al., 2019). Second, the technology, feedstock and other heterogeneities of individual units might result in the uncertainty for the use of uniform emission factors. Thus, the probability of emission factors was assumed to follow a normal distribution with a CV of 20% (Wang et al., 2019). A Monte Carlo approach was employed to generate random values for activity data and emission factors for each unit, and a total of 10,000 simulations were performed to estimate the uncertainty ranges of our estimates (Tang et al., 2019). The analysis results show that even with random variations, the emission estimation appears quite stable (with monthly emission factors and absolute emissions all varying within ±28.72%, in terms of 2 standard deviations) (Liu et al., 2015).

2.2. Air quality modelling

The CAMx model, a widely adopted photochemical dispersion model, was applied to investigate the impact of China's iron and steel industry emissions on the air quality in 2012. The CAMx model is a three-dimensional Eulerian-type regional air quality model, which simulates based on meteorological field and emission inventory. The emission inventory includes background emissions and target emissions (i.e., iron and steel industry emissions). Sections 2.2.1 and 2.2.2 illustrate the meteorological field and background emissions, respectively, and the air quality modelling is discussed in Section 2.2.3.

2.2.1. Meteorological data

In the air quality modelling, the Weather Research and Forecasting model (WRF 3.6) (Bo et al., 2019; ENVIRON, 2016; Wang et al., 2016a) was employed to simulate the meteorological field for 2012. There were 20 sigma levels within the planetary boundary layer, with a horizontal grid resolution of 36 km. The initial and boundary conditions for the simulation were generated using the final operational global analysis dataset (horizontal resolution 1° × 1°, 6-h interval) from the US National Center for Environmental Prediction and National Center for Atmosphere Research (Bo et al., 2019). The land use/cover and topographical data were derived from default WRF input dataset, at 30-second resolution.

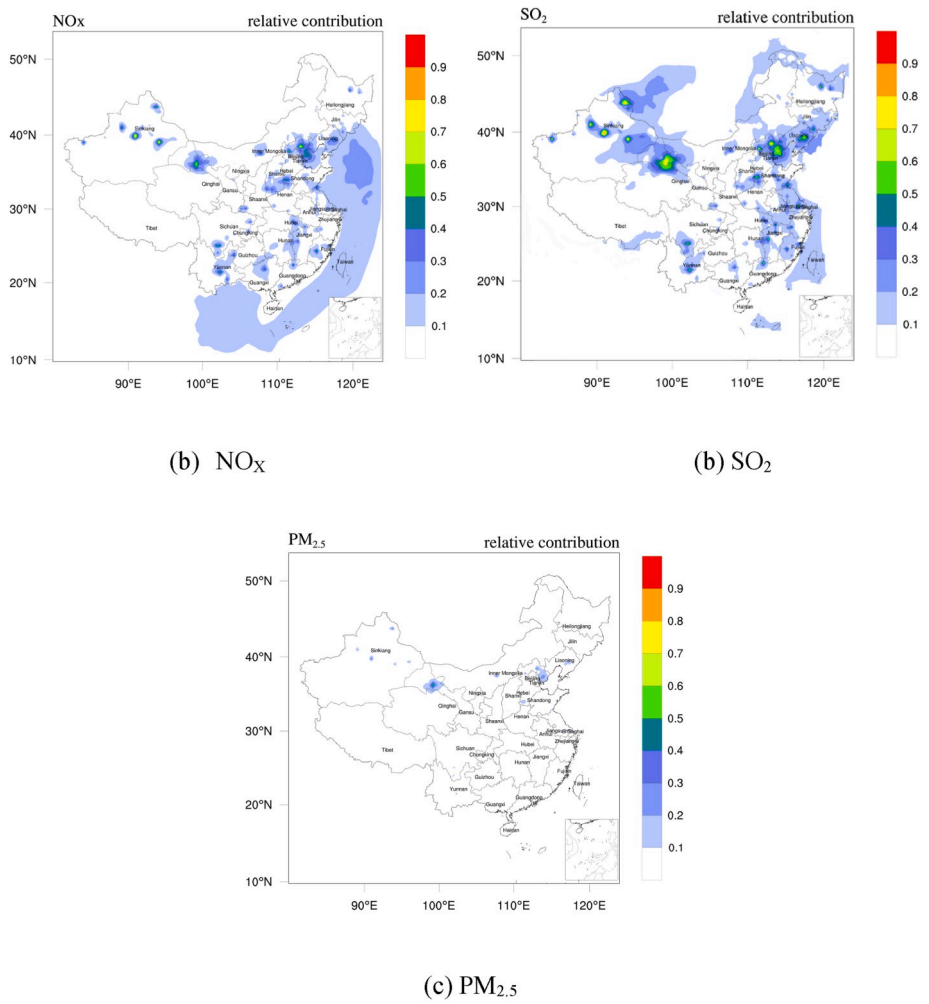


Fig. 7. Contribution of air pollutants emitted by China's iron and steel industry to ambient concentration in 2012 in terms of incremental rates (%).

2.2.2. *Background emissions*

The background emissions encompassed all anthropogenic and biogenic emissions, excluding estimated emissions from China's iron and steel industry. Anthropogenic emissions were derived from the Multi-resolution Emission Inventory for China, with a horizontal resolution of 0.25° × 0.25° (MEIC 1.2; http://www.meicmodel.org). Biogenic emissions were obtained from the Model of Emissions of Gases and Aerosols from Nature (MEGAN 2.0) (Guenther et al., 2006). All the emissions mentioned above were remapped as the input for CAMx model, through Sparse Matrix Operator Kernel Emissions (SMOKE 3.0) (UNC, 2005).

2.2.3. *Simulation*

CAMx (version 6.4) (Bo et al., 2019; Wang et al., 2016a) was employed in this research to quantify the air quality impact of emissions from China's iron and steel industry. As a three-dimensional Eulerian air quality numerical model, the CAMx provides an integrated analysis of transport of multiple air pollutants at various scales from regional to continental (Wang et al., 2016a). The domain (143 × 143 grid cells) area was centered at (110°E, 35°N), covering most areas of East Asia, with a grid resolution of 36 km. The vertical layer contained 20 sigma levels within 15-km altitude. Specific parameters of the other model settings (e.g., physical processes and chemical mechanisms) are presented in Table 3. A 10-day spin-up period was simulated to generate initial conditions, and the boundary condition was obtained from MOZART (a global chemistry transport model) (Bo et al., 2019). CF algorithm was employed to model aerosol processes, by dividing the size distribution into two static modes (coarse and fine) (Wang et al., 2016a). Primary species can be modeled as fine and/or coarse particles, while all secondary (chemically formed) species can only be modeled as fine particles. Greatly Reduced Execution and Simplified Dynamics (GREASD) plume-in-grid (PiG) option was used for the large point sources from the iron and steel industry in CAMx model (ENVIRON, 2016; Kemball-Cook et al., 2006).

To explore the impact of China's iron and steel industry emissions on the air quality, two scenarios were respectively simulated, as shown in Table 4. In each scenario, the related emission inventory, as well as meteorological field and environmental conditions, was taken as the model input file for CAMx. Thus, through the CAMx model, the volume-average species concentration of each grid were simulated according to Eulerian continuity equation, in which physical (e.g., transport) and chemical (e.g., interaction) process of multiple pollutants were considered simultaneously (Bo et al., 2019). Furthermore, the associated contribution of iron and steel industry emissions was quantified according to incremental concentrations (in $\mu g/m^3$) and incremental rates (%) under the scenarios with iron and steel industry emissions (i.e., S-1) relative to baselines without iron and steel industry emissions (i.e., S-0).

Since SO_2 and NOx are gas-phase species typically output in units of ppmV by CAMx model, we converted them from native model units to $\mu g/m^3$ through equation (4). In particular, the NOx indicates the combination of NO and NO_2.

$$C_s = C_{output,s} \times 1000 \times M_s/22.4, \quad (4)$$

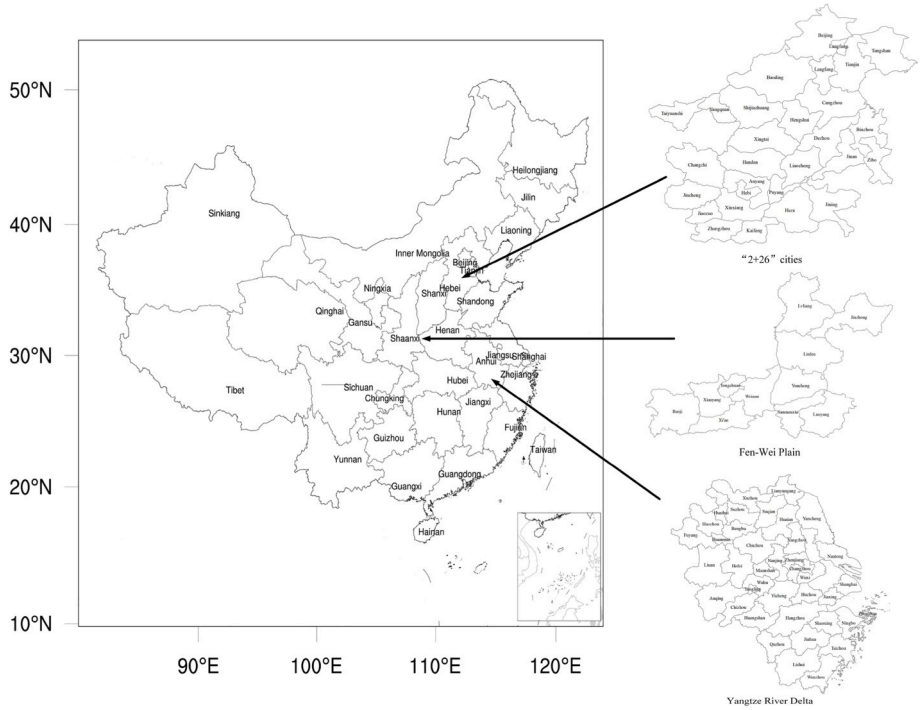


Fig. 8. Location for "2 + 26", the Fen-Wei Plain and the Yangtze River Delta in China.

where the subscripts *s* means the type of pollutant; C_s and $C_{output,s}$ indicate concentrations of each pollutant modeled by CAMx model, with unit of μg/m^3 and ppm, respectively; *M* represents molecular mass.

2.2.4. Model evaluation

For comprehensive evaluation of the WRF-CAMx model performance, we compared the observed and simulated values, in terms of meteorological factors (such as relative humidity, temperature and wind speed) and pollutant concentrations (e.g., PM_{10}, $PM_{2.5}$, SO_2 and NOx). For model evaluation, several statistical analyses were performed, in terms of the Pearson correlation coefficient (R), fractional bias (FB), normalized mean bias (NMB) and normalized mean error (NME), as illustrated in Table S13 in the SI.

Meteorological data were important inputs for the CAMx model. Based on previous research (Chen et al., 2019), major meteorological factors (such as temperature, relative humidity and wind speed) were employed to evaluate the accuracy of the WRF simulation. Therefore, we conducted a comparison analysis between observed and simulated meteorological factors at the daily level in 32 cities of China. The daily average monitoring data in 2012 were derived from the China Meteorological Administration (http://www.cma.gov.cn/). The detailed evaluations for each city are presented in Table S14, indicating the validity of the WRF performance.

For performance evaluation of CAMx model, monitoring data were compared with simulated values. On one hand, we compared daily observations with simulations for $PM_{2.5}$. Specifically, observed daily $PM_{2.5}$ concentrations were derived from the U.S. Department of State Air Quality Monitoring Program (available at http://www.stateair.net/web/historical), in which values for Beijing, Shanghai, Guangzhou and Chengdu were obtained for 2012. Table 5 presented comparison of daily observed concentrations for $PM_{2.5}$ with those of modelling, in terms of R, FB, NMB and NME.

On the other hand, we compared annual observations for pollutants (e.g., PM_{10}, SO_2 and NOx) with simulations of 144 cities. In detail, we obtain annual real air pollutant concentrations for these cities in 2012 from Environmental Statistics Bulletin. Statistical analyses were conducted to compare the annual simulations from the model and the observations at monitoring stations for four pollutants in the 144 cities at annual level, with results presented in Table 6.

Analysis of both daily and annual trend for these pollutants (Tables 6 and 7) indicates that simulated values were substantially consistent with the related observations. However, the simulated mean concentrations were slightly lower than observations in terms of NMB. The hidden reason is that not all actual emission sources are included, resulting in the underestimation of background emissions (Chen et al., 2019; Wang et al., 2016a). In addition, another potential reason might lie in the underestimates of secondary $PM_{2.5}$ concentrations. It could be attributed to the uncertainty in CAMx model mechanisms (e.g., the heterogeneous oxidation and wet scavenging processes) and the deficiency of certain process (e.g., oxidation of sulfur promoted by sea-salt and dust), which might result in the underestimation of the simulated sulfate (i.e., one of species of secondary $PM_{2.5}$) (Chen et al., 2019; Li et al., 2015; Wang et al., 2016a; Zhang et al., 2017).

2.3. Historical scenario

To evaluate the mitigation effect of current standards, we conducted a historical scenario for 1996 to compare the contribution of iron and industry emissions to ambient concentrations before and after the implementation of standards in 2012.

Two main steps were involved in this analysis. First, in the historical scenario for 1996, we estimated iron and steel industry emissions based on the emission factor method. In particular, the historical emission factors for different processes were estimated using Eq. (3) and concentrations were obtained from the standard GB 16297–1996 (i.e., standard implemented before 2012) (shown in Tables S1–S6 in the SI). In particular, the concentration calculations for pollutants of SO_2 and PM_{10} are based on the emission limit values of the standard GB 16297–1996, while those for NOx are still on the basis of 2012 standards. The hidden reason is that emission limit values for NOx were first set in new 2012 standards and at a high level; thus, the iron and steel industry can achieve compliance with 2012 standards at previous concentration levels. Then, the historical emissions were estimated based on Eq. (1). Notably, to reflect the impact of emission intensity changes (the

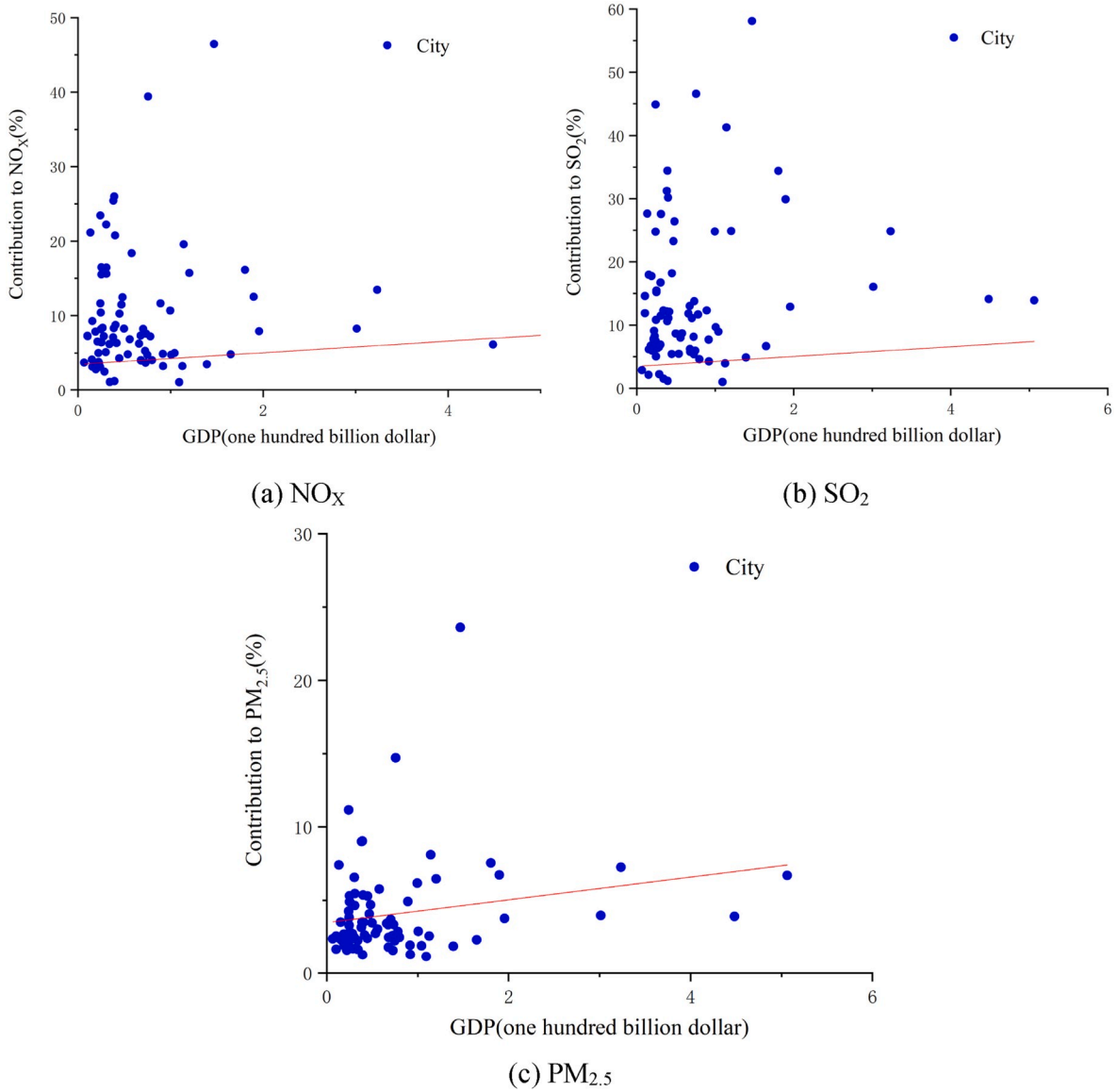


Fig. 9. China's iron and steel industry emissions for NOx (**a**), SO_2 (**b**) and $PM_{2.5}$ (**c**) with GDP for "2 + 26", the Fen-Wei Plain and the Yangtze River Delta in 2012.

targets of the current standards), this historical scenario shares the same activity level with current scenario. Second, we employed the CAMx model to simulate the contribution of iron and industry historical emissions to air quality, in which the meteorology data and background emissions were similar to those of 2012.

3. Results and discussions

Based on the two steps of the methodology described above, iron and steel industry emissions and contribution to the air quality in China were explored. In particular, a nationwide, unit-based inventory of China's iron and steel industry emissions was first constructed, with the analysis presented in Section 3.1. The corresponding contribution to the air quality concentrations was then simulated with the CAMx model, with the results discussed in Section 3.2. Finally, the air quality improvement associated with the current standards was revealed, with the discussion reported in Section 3.3.

3.1. Iron and steel industry emissions

China's iron and steel industry emissions in 2012 were estimated as follows: 1586.6 Gg SO_2, 1842.6 Gg NO_X, 682.0 Gg PM_{10} and 338.6 Gg $PM_{2.5}$. The estimation results for China's iron and steel industry emissions are next analyzed from spatial, process and temporal perspectives.

Concerning the spatial distribution, the nationwide and detailed emissions from China's iron and steel industry in 2012 are summarized in Fig. 2 and Fig. S1. Two insightful conclusions can be drawn from the results. China's iron and steel industry emissions vary considerably nationwide, with the highest emissions mainly located in certain areas. Hebei contributed to the largest shares of the SO_2 emissions (approximately 27.08% of total in 2012), closely followed by Liaoning (10.04%) and Jiangsu (8.91%), respectively. Hebei, Shandong and Jiangsu were the three largest contributors to NO_X emissions, with shares of 28.40%, 9.00% and 8.90%, respectively. Hebei had the largest contribution to PM_{10} and $PM_{2.5}$ emissions, (28.76% and 28.32%), followed by Jiangsu (8.64% and 9.11%) and Liaoning (8.50% and 8.40%), respectively. For other pollutants, Hebei contributed the largest portion of emissions (28.47%, 25.23%, 28.63%, 25.34% for PCDD/Fs, VOCs, CO and F, respectively), followed by Jiangsu (9.45%, 9.29%, 9.28% and 11.65%, respectively) and Shandong (9.10%, 8.91%, 9.08% and 8.39%, respectively). This unevenness in the emissions can be mainly attributed to the clear variations in the iron and steel production yields. Specifically,

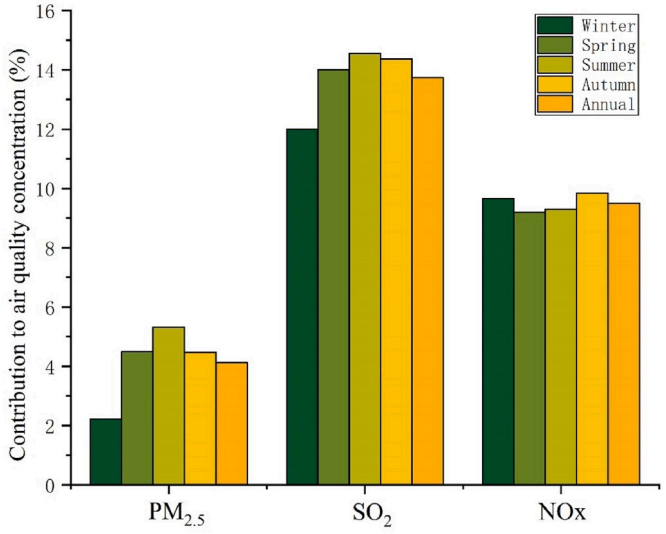
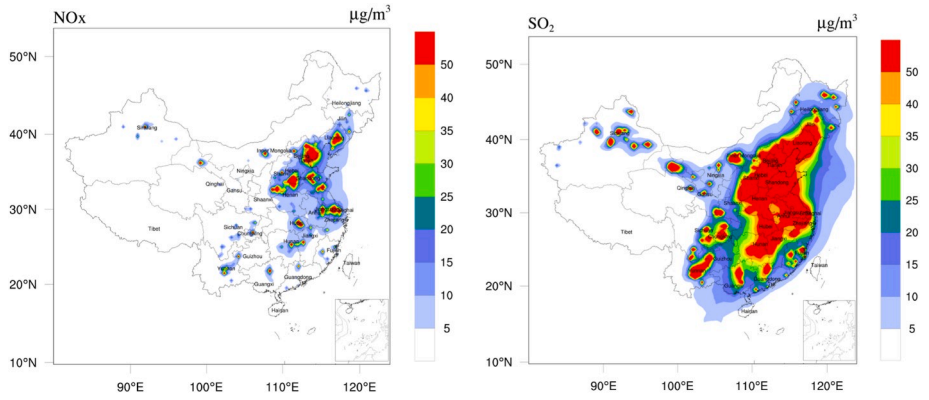


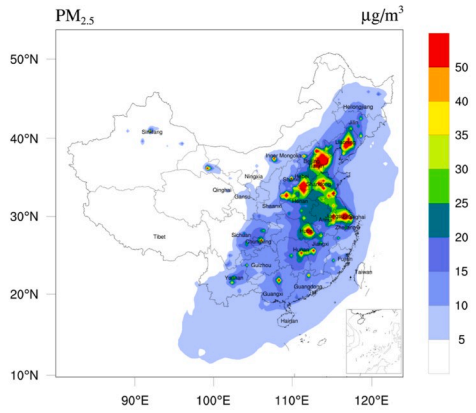
Fig. 10. Contribution of air pollutants emitted by China's iron and steel industry to air quality concentrations in 2012.

activity level is the main driving factor of emissions (see Eq. (1)) (Zheng et al., 2018), thus iron and steel industry emissions are generally consistent with the spatial distribution of crude steel production, with Pearson correlation coefficients over 0.99 for all of the aforementioned emission pollutants. In particular, together accounting for nearly 60% of the output of total nation crude steel, Hebei, Shandong, Jiangsu, Liaoning and Shanxi rank as the top 5 provincial emitters.

Fig. 3 illustrates the negative impact of economic level (GDP per capita) on China's iron and steel industry emission intensity (emission per crude steel output) at provincial level (detailed province information in Table S15). A linear regression is introduced, and t and F statistics both support this negative contribution statistically at a confidence level of 95% (Table 7). This could be attributed to the application of pollution control technology (Tong et al., 2018). The installation and operation of control technology cause an additional economic burden for the enterprises, resulting in a reduction of corporate profits (Yang et al., 2018). As economic level rises, enterprise investments for environmental improvements are expanded and thus applications of control technology are widely promoted, which could substantially reduce emission intensity (Tong et al., 2018). Notably, with developed economic level, installation rate of desulfurization technologies in Shanghai and Zhejiang were 85.65% and 89.17%, respectively, thus promoting a low-level emission intensity (0.81 and 1.44 kg/t, respectively). Notably, Tianjin, as the city with the highest per capita GDP in China in 2012, has the desulfurization rate and dust removal efficiency of 20.39% and 96.94%,



(c) NO_X (b) SO_2



(c) $PM_{2.5}$

Fig. 11. Contribution of air pollutants emitted by China's iron and steel industry to ambient concentration in historical scenario in terms of incremental concentrations (μg/m^3).

respectively, making for a relatively low emission-intensity (2.44 and 0.82 kg/t for SO_2 and $PM_{2.5}$). These areas of high emissions and emission intensity represent opportunities to conduct targeted air pollutant emission mitigation through the optimization and adjustment of regional iron and steel industrial structure and layout.

From a process perspective, Fig. 4 illustrates the contribution of multiple pollutant emissions divided by each iron and steel production processes for 2012. Overall, sintering and pelleting were the largest contributors for most pollutants, with more than 50% contribution on average. In contrast, contributions from electric furnace and rolled steel were less than 4% for all pollutants on average. In particular, sintering was the largest emitter of all of China's iron and steel production processes, contributing 69.52% of the total SO_2 emissions and 75.48%, 45.81%, 47.99% and 91.75% of NO_X, PM_{10}, $PM_{2.5}$ and PCDD/Fs emissions, respectively. Following sintering, coking was the largest contributor for VOC emissions (41.81% of total) and converter furnace yields the highest proportion for CO (37.79%) and fluoride (58.60%) emissions. Massive amounts of flue gas volume and high concentrations are produced during the thermal metallurgical process, leading to huge emissions being mainly discharged from sintering tail (Ren et al., 2014; Wang et al., 2019). Thus, a series of technological improvements can be applied to the sintering process, such as decreasing coke powder and introducing sintering additives (Ren et al., 2014). Against this background, targeting high-emission processes, particularly sintering and pelleting, is strongly recommended in emissions reduction, such as measurements of strengthening process emission standards, upgrading control technologies efficiency and improving feed material quality.

Concerning temporal evolution, Fig. 5 demonstrates the temporal trend of monthly emissions from China's iron and steel industry in 2012 by pollutants. Different pollutants generally show similar monthly emission patterns, indicating that monthly emission profiles of each are dominated by monthly variations in activity rates. In particular, the maximum value of annual total emissions of pollutants occurred in January (1586.6 Gg SO_2, 1842.6 Gg NO_X, 682.0 Gg PM_{10} and 338.6 Gg $PM_{2.5}$), while the minimum emissions occurred in February. The ratios of monthly multi-pollutant emissions between maxima and minima were within the range of 1.26–1.28. Moreover, the monthly variations in iron and steel emissions were generally consistent with those in industrial GDP in 2012 ($r = 0.62$). This suggests that economic levels are the main driving factor for production activity and thus dominate pollution behaviors (see Eq. (1)).

3.2. Air quality contribution

The contribution of emissions from China's iron and steel industry to air quality concentrations was explored with the CAMx model, and is presented by incremental concentrations (in $\mu g/m^3$) and incremental rates (%) from spatial, pollutants and temporal perspectives.

From the spatial distribution perspective, the contributions of China's iron and steel industry to air quality concentrations of major air pollutants in 2012 were analyzed (shown in Fig. 6 and Fig. 7). In terms of the contribution to air quality concentration in provincial level, China's iron and steel industry emissions mainly affected Hebei, Tianjin and Liaoning. The larger contributions of SO_2 emissions from iron and steel facilities to air quality concentrations were found in Hebei, Tianjin and Liaoning (33.42%, 29.84% and 29.68%, respectively) for regional air pollution. The larger contributions of NO_X emissions to air quality concentrations were found in Hebei, Yunnan and Hubei (23.59%, 22.21% and 19.91%, respectively). The larger contributions of $PM_{2.5}$ emissions to air quality concentrations were found in Hebei, Tianjin and Liaoning, accounting for 9.93%, 8.59% and 7.70%, respectively. The spatial distribution of emissions is dominated by the comprehensive impact of crude steel production (Wang et al., 2019) and air pollution control measurements coverage (Wu et al., 2015). In this study, the simulation results show that Hebei, Tianjin and Liaoning contributed the most greatly of the studied areas, because of their relatively large production of crude steel (18269.071, 1337.603 and 4893.868 million tons, respectively) and relatively low air pollution control measurements coverages (57.04%, 20.39% and 31.36%, respectively).

In particular, the contributions to air quality concentrations in the key areas, such as cities of "2 + 26" (Beijing-Tianjin-Hebei and surrounding areas) (MEE, 2017b), the Fen-Wei Plain and the Yangtze River Delta (with detailed information in Table S16 and Fig. 8), were especially concerned in the fight against air pollution in China. The contribution of China's iron and steel industry to the ambient environment in these areas in 2012 was analyzed. In "2 + 26" cities, China's iron and steel industry contributed greatly to the major air pollutant concentration of Tangshan (58.08%, 46.44% and 23.60% for SO_2, NO_X and $PM_{2.5}$, respectively), Handan (46.54%, 39.40% and 14.70%, respectively) and Anyang (34.38%, 25.97% and 9.03%, respectively). In the Fen-Wei Plain, emissions from the iron and steel industry contributed greatly to air quality in Linfen (58.08%, 46.44% and 23.60% for SO_2, NO_X and $PM_{2.5}$, respectively) and Lvliang (58.08%, 46.44% and 23.60%, respectively). In the Yangtze River Delta, Quzhou was the largest contributor (44.87%, 23.42% and 11.50% for SO_2, NO_X and $PM_{2.5}$, respectively), followed by Nantong (41.26%, 19.55% and 8.09%, respectively) and Nanjing (34.36%, 16.12% and 7.54%, respectively). Furthermore, Fig. 9 shows the contributions of the iron and steel industry emission to air quality, and shows a positive correlation with GDP in these key areas. This indicates that the iron and steel industry accelerates the economic level, but simultaneously leads to a great burden for environmental pollution.

From the pollutant perspective, this research mainly explored the contribution of SO_2, NO_X and $PM_{2.5}$ to air quality concentrations (Fig. 10). China's iron and steel industry contributed 13.73%, 9.50% and 4.13% to the annual mean concentration of SO_2, NO_X and $PM_{2.5}$, respectively. This indicates that among the three main pollutants, SO_2 made the main contribution to the regional air quality concentration. Against this background, there is still much room for improvement of SO_2 control and thus annual amount of SO_2 emission reductions are set for compulsory targets during 2010–2015 (MEE, 2010). Therefore, the installation of flue gas desulfurization for sintering increased from 20% in 2012 to 50% in 2015 and associated removal efficiencies increased by about 1.8-fold during 2012–2015 (Wang et al., 2019).

From the temporal perspective, the contribution of China's iron and steel industry to the air quality concentrations of major air pollutants was explored in different seasons, where January, April, July and October were selected to represent winter, spring, summer and autumn (Wang et al., 2016a) (Fig. 10). The simulation results show that the greatest contributions occurred in spring (14.55%, 9.30% and 5.32% for SO_2, NO_X and $PM_{2.5}$, respectively), whereas the lowest contributions were found in winter (12.0%, 9.65% and 2.22% for SO_2, NO_X and $PM_{2.5}$, respectively). This is first because heating is an important contributor to air pollution during winter, leading to considerable increases in emissions (Zhang et al., 2009). However, iron and steel industry emissions of pollutant change only slightly and thus, the contribution of China's iron and steel industry decreases. Second, the boundary layer is higher in summer, and the turbulent mixing effect causes better vertical mixing of the pollutants in summer, thus lowering concentrations at the surface (Duan et al., 2018).

3.3. Scenario analysis

For the historical scenario for 1996, the contribution of China's iron and steel industry to the annual mean concentration of major air pollutants is displayed in Fig. 11. Compared with the historical scenario, the current scenario reveals a striking downtrend for the contribution concentrations averaged across mainland China, with decreases of 92.07%, 72.91% and −14.38% for SO_2, $PM_{2.5}$, and NOx, respectively.

Such a substantial reduction in contributions is closely related to stricter limit values of the current standards, with levels of stringency surpassing the previous standards by up to 91% and 60% for SO_2 and

$PM_{2.5}$, respectively, across all processes. However, the limit values for NOx in iron and steel industries were implemented until 2012, and at a high level. Thus, it might be large potential improvement for NOx control for iron and steel industry in the future.

4. Conclusions

In general, this paper is the first attempt to simulate the contribution of China's iron and steel industry to air quality at the national scale. A high-resolution (i.e., unit-based, monthly-frequency, source-level and multi-pollutants) emissions inventory for iron and steel industry in 2012 was established, covering 1499 enterprises in China. This high-resolution emissions inventory was then introduced into the CAMx model, to systematically explore the contribution of these pollutant emissions to air quality. The simulation results indicated that: (1) from the spatial perspective, the air quality contributions were highly concentrated in eastern areas with high crude steel production; (2) among the pollutants, SO_2 made the largest contribution to air quality; (3) from the temporal perspective, the largest contribution to air quality concentrations occurred in summer, whereas the smallest contribution was found in winter; (4) from policy evaluation, the analysis results verified the efficacy of the current standards implemented in 2012, which resulted in a substantial reduction in contribution to air quality by 73%–92%.

Many topics require further investigation in future research. The empirical study can be further improved from the following perspectives. To explore systematic air quality improvement, the latest continuous emission monitoring systems (CEMS) data can be applied to further verify the validity of standards implication. In addition, the contribution of PCDD/Fs and F emissions to ambient concentration could be simulated by the CAMx model, which is an insightful extension to this study.

Declaration of competing interest

The authors declare that they have no known competing financial interests or personal relationships that could have appeared to influence the work reported in this paper.

CRediT authorship contribution statement

Ling Tang: Conceptualization, Methodology, Writing - original draft, Writing - review & editing. **Xiaoda Xue:** Formal analysis, Writing - original draft, Writing - review & editing. **Min Jia:** Formal analysis. **Hong Jing:** Investigation. **Tong Wang:** Writing - original draft. **Ruiqing Zhen:** Data curation. **Mantang Huang:** Software, Validation. **Jun Tian:** Software, Validation. **Jing Guo:** Formal analysis. **Ling Li:** Writing - review & editing, Visualization. **Xin Bo:** Conceptualization, Methodology, Supervision, Project administration. **Shouyang Wang:** Conceptualization, Methodology.

Acknowledgements

This work is supported by grants from the National Research Program for Key Issues in Air Pollution Control (No. DQGG0209-07 and DQGG0304-07), the National Natural Science Foundation of China (No. 71622011, 71971007 and 71988101), the National Program for Support of Top Notch Young Professionals, the National Key Research and Development Program of China (No. 2016YFC0208101) and the Appraisal Center for Environment and Engineering Ministry of Ecology and Environment (No. 2019–10).

Appendix A. Supplementary data

Supplementary data to this article can be found online at https://doi.org/10.1016/j.atmosenv.2020.117668.

References

Abdul-Wahab, S., Fadlallah, S., Al-Rashdi, M., 2018. Evaluation of the impact of ground-level concentrations of SO_2, NO_X, CO, and PM_{10} emitted from a steel melting plant on Muscat, Oman. Sustainable Cities and Society 38, 675–683.

Acciai, C., Zhang, Z., Wang, F., Zhong, Z., Lonati, G., 2017. Characteristics and source analysis of trace elements in $PM_{2.5}$ in the urban atmosphere of Wuhan in spring. Aerosol and Air Quality Research 17, 2224–2234.

Almeida, S.M., Lage, J., Fernández, B., Garcia, S., Reis, M.A., Chaves, P.C., 2015. Chemical characterization of atmospheric particles and source apportionment in the vicinity of a steelmaking industry. Sci. Total Environ. 521, 411–420.

Bo, X., Zhao, C.L., Wu, T., Su, Y., Wang, L.F., Tian, J., Shi, Y.L., Luo, M., Li, S., 2015. Emission inventory with high temporal and spatial resolution of steel industry in the Beijing-Tianjin-Hebei Region, 2015 China Environ. Sci. 35 (8), 2554–2560 (in Chinese).

Bo, X., Xu, J., Du, X.H., Guo, Q.Q., Zhen, R.Q., Tian, J., Cai, B.F., Wang, L.F., Ma, F.S., Zhou, B.H., 2017. Impacts assessment of steel plants on air quality over Beijing-Tianjin-Hebei area. China Environ. Sci. 37 (5), 1684–1692 (in Chinese).

Bo, X., Xue, X.D., Xu, J., Du, X.H., Zhou, B.H., Tang, L., 2019. Aviation's emissions and contribution to the air quality in China. Atmos. Environ. 201, 121–131.

Chen, R.J., Zhao, Z.H., Kan, H.D., 2013. Heavy smog and hospital visits in Beijing, China. Am. J. Respir. Crit. Care Med. 188 (9), 1170–1171.

Chen, Z.Y., Chen, D.L., Wen, W., Zhang, Y., Kwan, M.P., Chen, B., Zhao, B., Yang, L., Gao, B.B., Li, R.Y., Xu, B., 2019. Evaluating the "2+26" regional strategy for air quality improvement during two air pollution alerts in Beijing: variations in $PM_{2.5}$ concentrations, source apportionment, and the relative contribution of local emission and regional transport. Atmos. Chem. Phys. 19 (10).

Ciarelli, G., Aksoyoglu, S., Haddad, I.E., Bruns, E.A., Crippa, M., Poulain, L., Äijälä, M., Carbone, S., Freney, E.J., Dowd, C., Baltensperger, U., Prevot, A.S.H., 2017. Modelling winter organic aerosol at the European scale with CAMx: evaluation and source apportionment with a VBS parameterization based on novel wood burning smog chamber experiments. Atmos. Chem. Phys. 17 (12), 7653–7669.

Colella, P., Woodward, P., 1984. The piecewise parabolic method (PPM) for gas-dynamical simulations. J. Comput. Phys. 54, 174e201.

Coudon, T., Danjou, A.M.N., Faure, E., Praud, D., Severi, G., Mancini, F.R., Salizzoni, P., Fervers, B., 2019. Development and performance evaluation of a gis-based metric to assess exposure to airborne pollutant emissions from industrial sources. Environ. Health 18 (1), 8.

Dai, Q., Li, L., Yang, J., Liu, B., Bi, X., Wu, J., Zhang, Y., Yao, L., Feng, Y., 2016. The fractionation and geochemical characteristics of rare earth elements measured in ambient size-resolved PM in an integrated iron and steelmaking industry zone. Environ. Sci. Pollut. Control Ser. 23 (17), 17191–17199.

Di Gilio, A., Ventrella, G., Giungato, P., Tutino, M., Giua, R., Assennato, G., Gennaro, G., 2017. An intensive monitoring campaign of PAHs for assessing the impact of a steel plant. Chemosphere 168, 171–182.

Du, X., Xu, J., Liu, H.F., Liu, J., He, Y.J., Dang, H.Y., Meng, F., 2016. Contribution of power plant emissions to PM2.5 over Beijing-Tianjin-Hebei area during heavy pollution periods[J], 04 Res. Environ. Sci. 29, 475–482 (in Chinese).

Duan, W.J., Lang, J.L., Cheng, S.Y., Jia, J., Wang, X.Q., 2018. Air pollutant emission inventory from iron and steel industry in the Beijing-Tianjin-Hebei Region and its impact on $PM_{2.5}$, 04 Environmental Science 39, 1445–1454 (in Chinese).

Environ, 2016. User's guide to the comprehensive air quality model with extensions (CAMx). version 6.4. http://www.camx.com.

Fann, N., Baker, K.R., Fulcher, C.M., 2012. Characterizing the $PM_{2.5}$-related health benefits of emission reductions for 17 industrial, area and mobile emission sectors across the US. Environ. Int. 49, 141–151.

Guenther, A., Karl, T., Harley, P., Wiedinmyer, C., Palmer, P.I., Geron, C., 2006. Estimates of global terrestrial isoprene emissions using MEGAN (model of emissions of Gases and aerosols from nature). Atmos. Chem. Phys. 6 (11), 3181–3210.

Gulia, S., Kumar, A., Khare, M., 2015. Performance evaluation of CALPUFF and AERMOD dispersion models for air quality assessment of an industrial complex. J. Sci. Ind. Res. 74, 302–307.

Guo, Y., Gao, X., Zhu, T., Luo, L., Zheng, Y., 2017. Chemical profiles of PM emitted from the iron and steel industry in northern China. Atmos. Environ. 150, 187–197.

Guttikunda, S.K., Pant, P., Puja Jawahar, N.K.A., 2019. Particulate matter source contributions for Raipur-Durg-Bhilai region of Chhattisgarh, India. Aerosol and Air Quality Research 19, 528–540.

He, K.B., 2017. Technical Manual for the Preparation of Urban Air Pollutant Emission Inventory 2017. School of Environment, Tsinghua University, Beijing.

Ho, K.F., Ho, S.S.H., Huang, R.J., Chuang, H.C., Cao, J.J., Han, Y.M., Lui, K.H., Ning, Z., Chuang, K.J., Cheng, T.J., Lee, S.C., Hu, D., Wang, B., Zhang, R.J., 2016. Chemical composition and bioreactivity of PM2.5 during 2013 haze events in China. Atmos. Environ. 126, 162–170.

Huang, R.J., Zhang, Y., Bozzetti, C., Ho, K.F., Cao, J.J., Han, Y., Daellenbach, K.R., Slowik, J.G., Platt, S.M., Canonaco, F., 2014. High secondary aerosol contribution to particulate pollution during haze events in China. Nature 514 (7521), 218.

Jia, J., Cheng, S., Yao, S., Xu, T., Zhang, T., Ma, Y., Wang, H., Duan, W., 2018. Emission characteristics and chemical components of size-segregated particulate matter in iron and steel industry. Atmos. Environ. 182, 115–127.

Kemball-Cook, S., Johnson, J., Yarwood, G., 2006. Modeling Northeast Texas Ozone for Summer 2005. ENVIRON International Corporation, Novato, CA.

Kim, Y.H., Krantz, Q.T., McGee, M., Kovalcik, K., Duvall, R.M., Willis, R.D., Kamal, A.S., Landis, M.S., Norris, G., Gilmour, M.L., 2016. Chemical composition and source apportionment of size fractionated particulate matter in Cleveland, Ohio, USA. Environ. Pollut. 218, 1180–1190.

Lei, Y., 2008. Research on Anthropogenic Emissions and Control of Primary Particles and its Key Chemical Components. Tsinghua University, Beijing, China (in Chinese).
Lei, Y., Zhang, Q., He, K.B., Streets, D.G., 2011. Primary anthropogenic aerosol emission trends for China, 1990-2005. Atmos. Chem. Phys. 11 (3), 931.
Li, X., Nie, T., Qi, J., Zhou, Z., Sun, X.S., 2015. Regional source apportionment of $PM_{2.5}$ in beijing in january 2013[J], 04 Environmental Science 36, 1148–1153 (in Chinese).
Li, H., Wang, Y., Li, H., Zhu, C., Mao, H., Yang, M., Wang, R., Wang, W., 2016. Investigation of sources of atmospheric polycyclic aromatic hydrocarbons at Mount Lushan in southern China. J. Geophys. Res.: Atmosphere 121 (6), 3050–3061.
Li, M., Zhang, Q., Kurokawa, J.I., Woo, J.H., He, K., Lu, Z., Ohara, T., Song, Y., Streets, D. G., Carmichael, G.R., Cheng, Y., Hong, C., Huo, H., Jiang, X., Kang, S., Liu, F., Su, H., Zheng, B., 2017. MIX: a mosaic Asian anthropogenic emission inventory under the international collaboration framework of the MICS-Asia and HTAP. Atmos. Chem. Phys. 17 (2).
Liu, Z., Guan, D., Wei, W., Davis, S.J., Ciais, P., Bai, J., Peng, S., Zhang, Q., Hubacek, K., Marland, G., Andres, R.J., Crawford-Brown, D., Lin, J., Zhao, H., Hong, C., Boden, T. A., Feng, K., Peters, G.P., Xi, F., Liu, J., Li, Y., Zhao, Y., Zeng, N., He, K., 2015. Reduced carbon emission estimates from fossil fuel combustion and cement production in China. Nature 524 (7565), 335–338.
Liu, H., Wu, B., Liu, S., Shao, P., Liu, X., Zhu, C., Wang, Y., Yu, Y., Xue, Y., Gao, J., Hao, Y., Tian, H., 2018. A regional high-resolution emission inventory of primary air pollutants in 2012 for Beijing and the surrounding five provinces of North China. Atmos. Environ. 181, 20–33.
Ministry of Ecological Environment of the People's Republic of China (MEE), 2010. Guidelines for Establishment of the 12th Five-Year Plan for Total Emission Control of Major Pollutants (in Chinese).
Ministry of Ecological Environment of the People's Republic of China (MEE), 2014. Technical Guide for Compiling Emission Inventory of Atmospheric Volatile Organic Compounds (On Trial) (in Chinese).
Ministry of Ecology and Environment of the People's Republic of China (MEE), 2016. China Environmental Statistical Yearbooks 2015. Chinese Environmental Science Press, Beijing (in Chinese).
Ministry of Ecological Environment of the People's Republic of China (MEE), 2017a. Technical Specification for Application and Assurance of Pollutant Permit Iron and Steel Industry. Chinese Environmental Science Press, Beijing (in Chinese).
Ministry of Ecological Environment of the People's Republic of China (MEE), 2017b. 2017 Air Pollution Prevention and Management Plan for the Beijing-Tianjin-Hebei Region and its Surrounding Areas.
Foreign Economic Cooperation office of Ministry of Environmental Protection (MEPFECO), 2007. The people's Republic of China implementation schedule for stockholm convention on pops (in Chinese) [Available on the Internet at. htt p://www.mepfeco.org.cn/zyxx/cbw/fqk/200904/P020110718406770444112.pdf.
National Bureau of Statistics (NBS), 2013. China statistical database. available at: http://data.stats.gov.cn/.
National Development and Reform Commission (NDRC), 2013. Catalogue for Guiding Industry Restructuring, 2011.
Nenes, A., Pandis, S., Pilinis, C., 1998. ISORROPIA: a new thermodynamic equilibrium model for multiphase multicomponent inorganic aerosols. Aquat. Geochem. 4 (1), 123–152.
Ren, Z.P., Zhu, T.L., Zhu, T.Y., Dong, L., 2014. NOx and SO_2 formation in the sintering process and influence of sintering material composition on NOx emissions. Environment Science 35 (10), 3669–3673.
Salameh, T., Sauvage, S., Afif, C., Borbon, A., Locoge, N., 2016. Source apportionment vs. emission inventories of non-methane hydrocarbons (NMHC) in an urban area of the Middle East: local and global perspectives. Atmos. Chem. Phys. 16 (5), 3595–3607.
Shen, J., Wang, X.S., Li, J.F., Li, Y.P., Zhang, Y.H., 2011. Evaluation and intercomparison of ozone simulations by models-3/CMAQ and CAMx over the pearl River Delta. SCIENCE CHINA Chem 54 (11), 1789–1800.
Shutt, R.H., Kauri, L.M., Weichenthal, S., Kumarathasan, P., Vincent, R., Thomson, E.M., Liu, L., Mahmud, M., Cakmak, S., Dales, R., 2017. Exposure to air pollution near a steel plant is associated with reduced heart rate variability: a randomised crossover study. Environ. Health 16 (1), 4.
Song, Y., Zhang, M.S., Cai, X.H., 2006. PM_{10} modeling of Beijing in the winter. Atmos. Environ. 40 (22), 4126–4136.
Taiwo, A.M., Beddows, D.C.S., Calzolai, G., Harrison, R.M., Lucarelli, F., Nava, S., Shi, Z., Valli, G., Vecchi, R., 2014. Receptor modelling of airborne particulate matter in the vicinity of a major steelworks site. Sci. Total Environ. 490, 488–500.
Tan, J., Zhang, Y., Ma, W., Yu, Q., Wang, J., Chen, L., 2015. Impact of spatial resolution on air quality simulation: a case study in a highly industrialized area in Shanghai, China. Atmospheric Pollution Research 6 (2), 322–333.
Tan, J., Zhang, L., Zhou, X., Duan, J., Li, Y., Hu, J., He, K., 2017. Chemical characteristics and source apportionment of $PM_{2.5}$ in Lanzhou, China. Sci. Total Environ. 601, 1743–1752.
Tang, L., Qu, J., Mi, Z., Bo, X., Chang, X., Anadon, L.D., Wang, S., Xue, X., Li, S., Wang, X., Zhao, X., 2019. Substantial emission reductions from Chinese power plants after the introduction of ultra-low emissions standards. Nature Energy 4 (11), 929–938.
Tesche, T.W., Morris, R., Tonnesen, G., Mcnally, D., Boylan, J., Brewer, P., 2006. Cmaq/camx annual 2002 performance evaluation over the eastern us. Atmos. Environ. 40 (26), 4906–4919.
Tong, D., Zhang, Q., Davis, S.J., Liu, F., Zheng, B., Geng, G., Xue, T., Li, M., Hong, C., Lu, Z., Streets, D.G., Guan, D., He, K., 2018. Targeted emission reductions from global super-polluting power plant units. Nature Sustainability 1 (1), 59.
UNC Carolina Environmental Program, 2005. Sparse Matrix Operator Kernel Emissions (SMOKE) Modeling System. UNC Chapel Hill, North Carolina, USA.
Wang, J., Xu, J., He, Y., Chen, Y., Meng, F., 2016a. Long range transport of nitrate in the low atmosphere over Northeast Asia. Atmos. Environ. 144, 315–324.
Wang, K., Tian, H., Hua, S., Zhu, C., Gao, J., Xue, Y., Hao, J., Wang, Y., Zhou, J., 2016b. A comprehensive emission inventory of multiple air pollutants from iron and steel industry in China: temporal trends and spatial variation characteristics. Sci. Total Environ. 559, 7–14.
Wang, X., Yan, L., Lei, Y., He, K., He, J., 2016c. Estimation of primary particulate emissions from iron and steel industry in China. Acta Sci. Circumstantiae 36 (8), 3033–3039 (in Chinese).
Wang, X.Y., Lei, Y., Yan, L., Liu, T., Zhang, Q., He, K., 2019. A unit-based emission inventory of SO_2, NOx and PM for the Chinese iron and steel industry from 2010 to 2015. Sci. Total Environ. 676, 18–30.
Wen, J., Yang, J.M., Li, P., Yu, J., Wu, J.H., Tian, Y.Z., Zhang, J.S., Shi, G.L., Feng, Y.C., 2018. Chemical source profiles of PM emitted from the main processes of the iron and steel industry in China. Environmental Science 39 (11), 4885–4891.
Wesely, M.L., 1989. Parameterization of surface resistances to gaseous dry deposition in regional-scale numerical models. Atmos. Environ. 23, 1293–1304.
World Steel Association (WSA), 1990–2019. World Steel Statistical Yearbook (1997–2019 Version) (Brussels, Belgium).
Wu, X.C., Zhao, L.J., Zhang, Y.X., Zheng, C.H., Gao, X., Cen, K.F., 2015. Primary air pollutant emissions and future prediction of iron and steel industry in China. Aerosol and Air Quality Research 15 (4), 1422–1432.
Wu, Q., Gao, W., Wang, S., Hao, J., 2017. Updated atmospheric speciated mercury emissions from iron and steel production in China during 2000-2015. Atmos. Chem. Phys. 17, 10423–10433.
Yang, H., Zhang, Y., Zheng, C., Wu, X., Chen, L., Fu, J.S., Gao, X., 2018. Cost estimate of the multi-pollutant abatement in coal-fired power sector in China. Energy 161, 523–535.
Zhang, G., 2015. Emission Characteristics of Particulate Matter of Steel Plants. Northeastern University, Liaoning, China (in Chinese).
Zhang, Q., Streets, D.G., Carmichael, G.R., He, K., Huo, H., Kannari, A., Klimont, Z., Park, I., Reddy, S., Fu, J., 2009. Asian emissions in 2006 for the NASA INTEX-B mission. Atmos. Chem. Phys. 9 (14), 5131–5153.
Zhang, T.H., Chen, B.Z., Wang, J., Huang, C., Chen, L., Zhang, Z., 2017. Process analysis and source apportionment of $PM_{2.5}$ pollution in Xuzhou in winter 2016 based on CAMx. Acta Sci. Circumstantiae 37 (10), 3918–3925 (in Chinese).
Zhao, Y., Nielsen, C.P., Lei, Y., McElroy, M.B., Hao, J., 2011. Quantifying the uncertainties of a bottom-up emission inventory of anthropogenic atmospheric pollutants in China. Atmos. Chem. Phys. 11 (5), 2295–2308.
Zhao, B., Wang, P., Ma, J.Z., Zhu, S., Pozzer, A., Li, W., 2012. A high-resolution emission inventory of primary pollutants for the Huabei region, China. Atmos. Chem. Phys. 12 (1), 481–501.
Zhao, B., Amann, M., Fu, K., Hao, J.M., Wang, S., Xu, J., Klimont, Z., He, K.B., Cofala, J., 2013. NOx emissions in China: historical trends and future perspectives. Atmos. Chem. Phys. 13 (19), 9869–9897.
Zheng, B., Tong, D., Li, M., Liu, F., Hong, C., Geng, G., Li, H., Li, X., Peng, L., Qi, J., Yan, L., Zhang, Y., Zhao, H., Zheng, Y., He, K., Zhang, Q., 2018. Trends in China's anthropogenic emissions since 2010 as the consequence of clean air actions. Atmos. Chem. Phys. 18 (19), 14095–14111.
Zhu, Y.H., Li, H.L., Chen, J.Y., Jiang, F.T., 2019. Pollution control efficiency of China's iron and steel industry: evidence from different manufacturing processes. J. Clean. Prod. 240.